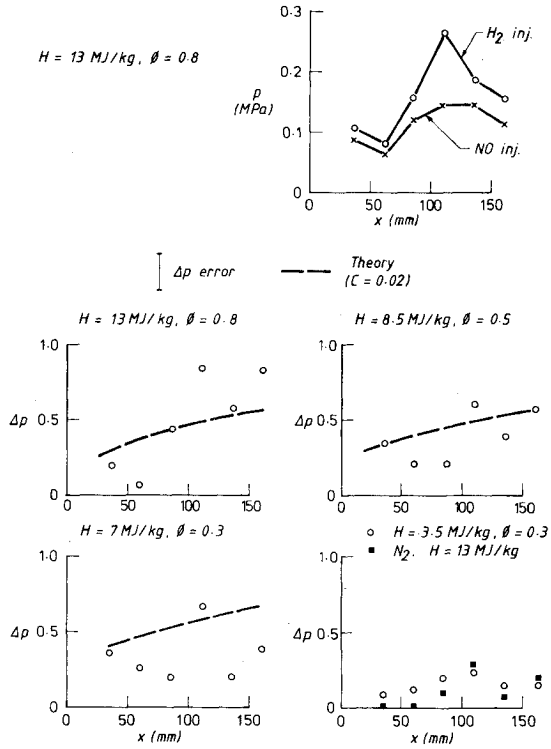

Fig. 2 Combustion-induced pressure distributions (H = stagnation enthalpy, x = distance downstream of injector).

constant at the freestream value, the velocity profile was linear from the centerline to the edge of the jet, and the turbulent eddy viscosity was given by

$$\epsilon = C\delta(u_e - u_m)$$

where u_e and u_m are freestream and centerline velocities, respectively, and C is a constant. At the edge of the jet, δ was put equal to half the width of the jet, and midway between the edge and the center, equal to 0.25 of half the width. The actual density distribution was then calculated by assuming that the Schwab-Zeldovich variables $[c_H + (C_pT + \frac{1}{2}u^2)/\Delta H]$, $(c_O + 8c_H)$, and $(c_O + 0.89\ C_w)$ varied linearly with the velocity. Here T and u are the temperature and velocity; C_p is the specific heat at constant pressure; ΔH is the heat of combustion; and c_H, c_O, and C_w are the mass fractions of H_2, O_2, and H_2O, respectively. Using this density together with the Howarth transformation, it was possible to calculate the displacement thickness of the jet and then, by assuming one-dimensional flow outside the jet, to make an estimate of the pressure rise associated with this displacement thickness.

As a check on the validity of this model, it was used to calculate the fringe shift profile across the jet, as observed by the interferometer at a station 33 mm downstream of the injector. Results are compared with experiment in Fig. 1. The fringe shift profile is adequately predicted for injection into nitrogen flow, when no reactions occur, but when combustion takes place, the strong negative fringe shift that is predicted near the flame front does not occur. As shown in the figure, better agreement can be obtained when dissociation of H_2O in this region is taken into account, especially when it is remembered that the discontinuous change in velocity gradient at the edge of the jet, which is assumed by the theory, is smoothed out to a more gradual change in practice. Taking account of H_2O dissociation changed the displacement thickness by less than 10%, and so this effect was ignored in the calculations.

The pressure distributions calculated by this analysis are presented in Fig. 2. The value of 0.02 for C was suggested by examination of low-speed data,[5] but the results indicate that, at least when the hydrogen injection velocity is much less than that of the freestream, as in these experiments, the same value may be used to obtain rough estimates of jet combustion behavior at high speeds.

Acknowledgment

This work was supported by the Australian Research Grants Committee.

References

[1] Bangert, L. H. and Sechacker, D. I., "Some Effects of Combustion on Turbulent Mixing," *AIAA Journal*, Vol. 14, March 1976, pp. 394-396.

[2] Stalker, R. J., "Development of a Hypervelocity Wind Tunnel," *Aeronautical Journal of the Royal Aeronautical Society*, Vol. 74, June 1970, pp. 374-384.

[3] Ferri, A., "Mixing—Controlled Supersonic Combustion," *Annual Review of Fluid Mechanics*, Vol. 5, Annual Reviews Inc., Palo Alto, Calif., 1973, pp. 301-338.

[4] Kanury, A. M., *Introduction to Combustion Phenomena*, Gordon and Breach, New York, 1977, pp. 222-225.

[5] Schlichting, H., *Boundary Layer Theory*, 6th ed., McGraw-Hill, New York, 1968, p. 698.

AIAA 82-4240

Curvature Effects on Heat Transfer in the Free Jet Boundary

Isaac W. Diggs*
Goodyear Atomic Corporation, Piketon, Ohio
and
Kenneth H. Kim†
University of Tennessee, Knoxville, Tenn.

Introduction

A GREAT deal of attention has been given to free jet flows where a pressure differential across the flow profile causes the stream to curve and attach itself to an adjacent wall. Such behavior by the jet is commonly referred to as the "Coanda" effect in fluidic devices, but these fields are also known to exist in flows associated with velocity discontinuities around airfoils. Instances exist as well where high temperatures and thermal radiation can be evident in these flows so that it would be of interest to discover how heat transfer capabilities in the thermal boundary layer are affected by curvature.

A physical interpretation of the steady, two-dimensional, incompressible flowfield and the boundary conditions which apply can be visualized as follows. The moving fluid which has already established a fully developed flow profile possesses a freestream velocity U_{max} and a bulk fluid temperature T_∞ before it reaches a region of stagnant fluid, which has velocity $u=0$ and a bulk fluid temperature T_s. A short distance, x_0, beyond this point of issue where the curvature is R_0, entrainment of the stagnant fluid causes alteration of the velocity and temperature profiles such that at large negative values of y ($y \to -\infty$), $u=0$ and $T=T_s$.

Received April 20, 1981; revision received March 4, 1982.
Copyright © American Institute of Aeronautics and Astronautics, Inc., 1982. All rights reserved.

*Staff Physicist, Gas Centrifuge Enrichment Plant Production Division.

†Associate Professor, Engineering Science and Mechanics.

Alternately, at large positive values of y $(y \to +\infty)$, freestream conditions again prevail. Constant curvature along the major streamline,[1-3] which serves as the abscissa in the curvilinear coordinate system, provides that the velocity normal to the direction of flow (v) is also zero at this point.

Analysis

Williams et al.[1] have provided a similarity analysis for laminar and turbulent velocity profiles that can be applied to this problem. They used the transformation parameters

$$\psi = (U_1 \nu x)^{1/2} f(\eta) \quad \text{with} \quad \eta = y(U_1/\nu x)^{1/2}$$

where $R = (R_0/x)^{1/2}$ for the laminar case, and

$$\psi = 1/2^{1/2}[(x/\omega)U_1 f(\eta)] \quad \text{with} \quad \eta = 2^{1/2}(\omega/x)y$$

where $R = R_0/x$ for the turbulent case. Both sets of transformation parameters produce a transformed differential equation of the form

$$2f'^{v} + f'f'' + ff''' + \Re(f'^2 + 2\eta f'f'') = 0 \tag{1a}$$

with the transformed boundary conditions being given by

$$f(0) = 0, \quad \lim_{\eta \to -\infty} f'(\eta) = 0 \quad \text{and for large } \eta_+ : \ f''/f' = -\Re \tag{1b}$$

The similarity curvature parameter is given by

$$\Re = (R_0 \nu / U_1)^{1/2} \quad \text{and} \quad \Re = R_0 \omega / 2^{1/2}$$

for the laminar and turbulent cases, respectively.

The Rosseland approximation for the radiative heat flux in an optically thick medium,[4] given by the expression

$$q_r = \frac{-4\lambda^2 \sigma}{3\kappa} \frac{\partial T^4}{\partial y}$$

can be used in the energy equation to provide the relation for which a solution is sought, namely,

$$\rho C_p \left(u \frac{\partial T}{\partial x} + v \frac{\partial T}{\partial y} \right) = K \frac{\partial^2 T}{\partial y^2} + \frac{4\lambda^2 \sigma}{3\kappa} \frac{\partial^2 T^4}{\partial y^2} \tag{2}$$

Laminar Flowfields

If it is assumed, as before, that the similarity stream function ψ is still valid, and T^4 is linearized through expansion about T_∞, the transformed energy equation can be nondimensionalized using the Prandtl number, conduction-to-radiation parameter, and dimensionless temperature. These are, respectively,

$$Pr = \frac{\nu}{\alpha}, \quad N = \frac{\kappa K}{4\lambda^2 \sigma T_\infty^3}, \quad \theta = \frac{T(\eta) - T_s}{T_\infty - T_s}$$

so that the resulting expression becomes

$$\left(1 + \frac{4}{3N}\right)\theta'' + \frac{Prf}{2}\theta' = 0 \tag{3a}$$

with boundary conditions

$$\lim_{\eta \to -\infty} \theta = 0, \quad \theta' = 0, \quad \lim_{\eta \to +\infty} \theta = 1, \quad \theta' = 0 \tag{3b}$$

Turbulent Flowfields

Introduction of the turbulent eddy viscosity ϵ, turbulent conductivity π, and turbulent Prandtl number, which are given by[1,5]

$$\epsilon = czxU_{\max} = A_\tau/\rho, \qquad \pi = C_p A_q, \qquad P_t = A_\tau / A_q$$

will provide the means to transform the energy equation. A_τ and A_q above are conductivity and viscosity constants dependent upon the level of turbulence in the flow. Evaluation of the mixing length constant cz and the free constant ω^2 as $1/729$ and $729U_1/U_{\max}$, respectively,[1] yields the following result after nondimensionalizing in a manner similar to that used in Eqs. (3a) and (3b):

$$\left(1 + \frac{4}{3N}\right)\theta'' + \frac{P_t f}{2}\theta' = 0 \tag{4}$$

with boundary conditions identical to those in Eq. (3b).

Discussion of Results

When no radiative contribution to the thermal boundary layer is evident ($N = \infty$), increases in $\Re$ cause an accompanying increase in the extent of the boundary layer

Table 1 Thermal boundary layer data comparison

	Data set No.	$\theta(0)$	$+\eta_{edge}$	θ_{edge}	$\theta'(0)$	$\Re$
$N=\infty$	1	0.586	4.100	0.99861E+0	0.26080E+0	0.0
	2	0.586	4.100	0.99863E+0	0.26077E+0	1.0×10^{-3}
	3	0.586	4.100	0.99823E+0	0.26051E+0	1.0×10^{-2}
	4	0.586	4.400	0.99751E+0	0.25986E+0	4.0×10^{-2}
	5	0.587	4.800	0.99700E+0	0.25841E+0	1.0×10^{-1}
$N=1.0$	1	0.631	6.000	0.99745E+0	0.15657E+0	0.0
	2	0.631	6.000	0.99757E+0	0.15655E+0	1.0×10^{-3}
	3	0.631	6.100	0.99856E+0	0.15627E+0	1.0×10^{-2}
	4	0.631	6.500	0.10014E+1	0.15560E+0	4.0×10^{-2}
	5	0.629	7.000	0.10013E+1	0.15366E+0	1.0×10^{-1}
$N=0.5$[a]	1	0.661	7.900	0.99697E+0	0.11610E+0	0.0
	2	0.661	7.400	0.99806E+0	0.11608E+0	1.0×10^{-3}
	2*	0.660	7.900	0.99738E+0	0.11590E+0	1.0×10^{-3}
	3	0.660	7.700	0.10011E+1	0.11568E+0	1.0×10^{-2}
	3*	0.655	14.800	0.99683E+0	0.11477E+0	1.0×10^{-2}
	4	0.655	8.600	0.10012E+1	0.11412E+0	4.0×10^{-2}
	4*	0.650	10.800	0.99704E+0	0.11329E+0	4.0×10^{-2}
	5	0.649	9.500	0.10007E+1	0.11186E+0	1.0×10^{-1}

[a] Data sets shown with asterisks (*) denote those which were calculated using overlap conditions to show transition from one value of $\Re$ to the next.

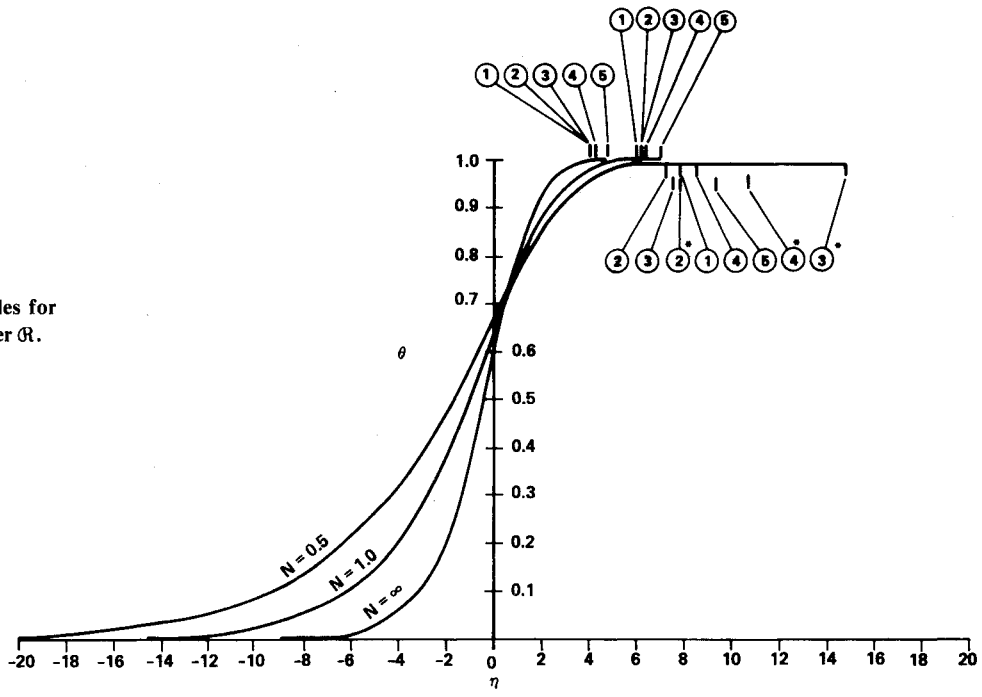

Fig. 1 Temperature profiles for varying curvature parameter $\Re$.

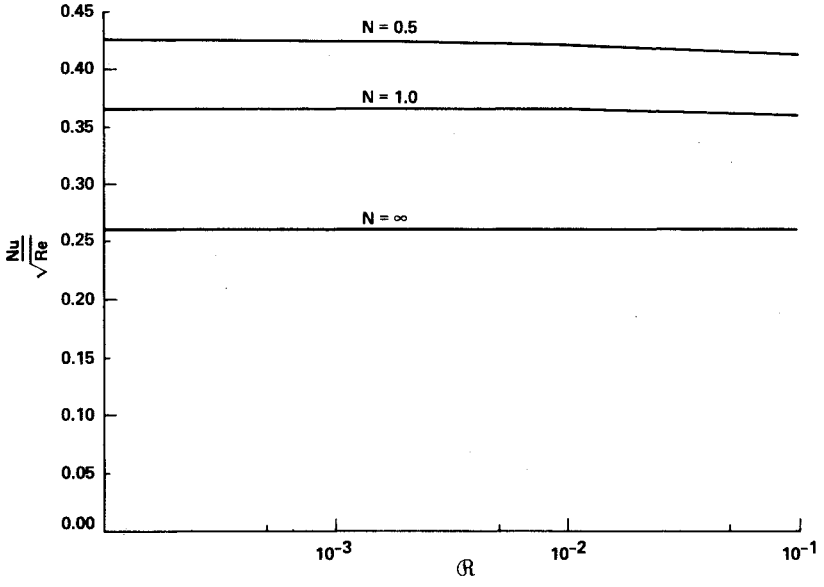

Fig. 2 Variation of $Nu/\sqrt{Re}$ with curvature parameter $\Re$.

toward the freestream, as indicated by the values for $+\eta_{edge}$ in Table 1. It would be well to remark here that solution of the nondimensionalized momentum and energy equations involved a three-point boundary condition, one each given in the problem statement for $+\infty$ and $-\infty$, and one chosen at $\eta=0$ and adjusted in a manner to assure satisfaction of the given constraints within a desired limit of error.[6] Thus it is inferred from the data in Table 1 that the increase in the major streamline temperature, $\theta(0)$, was necessary to assure that the other stated boundary conditions are met.

In the examination of data for equal conductive and radiative effects ($N=1.0$), the trend of boundary-layer extension with increased curvature is again evident. The overall thickness of the boundary layer without regard to curvature is also seen to be greater than for the case where $N=\infty$. An opposite effect on the major streamline temperature is evidenced in the limit of extreme curvature, however, as this value is shown to decrease.

The radiative boundary layer ($N=0.5$) displays a sensitivity to curvature that grows more pronounced as the value of $\Re$ increases. This condition required special treatment in order to establish a trend. An overlapping technique taking advantage of the error limit set on the value of $\theta(0)$ was employed by determining θ_{edge} with two slightly different values of $\theta(0)$ for each given $\Re$ between 0.0 and 1.0×10^{-1}. Therefore, the asterisked data sets in the table represent situations where transitions from one value of $\Re$ to the next larger one are accomplished by "overlapping" the error bound for the respective unasterisked data set (i.e., data set 2* overlaps data set 2 within $\pm\Delta\theta$ to satisfy asymptotic boundary condition). This method produces some fluctuation in the values for $+\eta_{edge}$, but the trend of decrease in boundary-layer thickness with increase in $\Re$ is clearly evident if one studies the data relative to what occurs across the overlap regions. The observed result is opposite to that obtained for either situation where $N=\infty$ or $N=1.0$. Figure 1 is a graphic comparison of temperature profiles for all three values of N reported in the tabulated data.

Results in Fig. 2 showing the Nusselt number to Reynolds number ratio,

$$\frac{Nu}{\sqrt{Re}}=\left(1+\frac{4}{3N}\right)\theta'(0) \tag{5}$$

as a function of curvature indicate that curvature affects heat flux across the major streamline very little. In fact, the curve for $N = \infty$ is nearly flat and the curves for $N = 1.0$ and 0.5 also show very nearly linear relationships, except in the region of curvature between 10^{-2} and 10^{-1}.

Summary

The results can be explained in part through examination of the transport processes evident in the flow. Study of the velocity profiles provided in Ref. 1 indicates that fluid motion in the jet boundary decreases more sharply toward the freestream as more severe curvature constraints are placed on the system. When conduction is predominant, the slower-moving fluid will have an adverse effect on convective transfers toward the stagnation region with a resulting decrease in the heat transfer across the major streamline and increase in boundary layer depth. If curvature constraints are severe, wall attachment of the jet could cause enhanced mixing of the two fluid layers, in effect raising the stagnation temperature from the vantage point of the major streamline and forcing a resultant temperature rise at the major streamline.

In the case of predominant radiation, the subsequent reductions of temperature gradient and heat flux across the major streamline can once again be explained with effects of curvature on convective transfers. Lowered velocities in the flowfield reduce the capability for fluid particles to interact. The restrictions inherent in the optically thick approximation require that decreased fluid mobility retard emission and absorption of thermal radiation, which would obviously reduce the extent of the thermal boundary layer.

References

[1] Williams, J. C., Cheng, E. H., and Kim, K. H., "Curvature Effects in the Laminar and Turbulent Freejet Boundary," *AIAA Journal*, Vol. 9, April 1971, pp. 733-736.

[2] Sawyer, R. A., "The Flow Due to a Two-Dimensional Jet Issuing Parallel to a Flat Plate," *Journal of Fluid Mechanics*, Vol. 9, Dec. 1960, pp. 543-561.

[3] Sawyer, R. A., "Two-Dimensional Reattaching Jet Flows Including the Effects of Curvature on Entrainment," *Journal of Fluid Mechanics*, Vol. 17, Dec. 1963, pp. 481-498.

[4] Viskanta, R. and Grosh, R. J., "Boundary Layer in Thermal Radiation Absorbing and Emitting Media," *International Journal of Heat and Mass Transfer*, Vol. 5, March 1962, pp. 795-806.

[5] Schlichting, H., *Boundary Layer Theory*, 4th ed., McGraw-Hill, New York, 1960.

[6] Nachtsheim, P. R. and Swigert, P., "Satisfaction of Asymptotic Boundary Conditions in Numerical Solution of Systems of Nonlinear Equations of Boundary Layer Type," NASA TN D-3004, Oct. 1965.

New Procedure for Submission of Manuscripts

Authors please note: Effective immediately, all manuscripts submitted for publication should be mailed directly to the Editor-in-Chief, *not* to the AIAA Editorial Department. Read the section entitled "Submission of Manuscripts" on the inside front cover of this issue for the correct address. You will find other pertinent information on the inside back cover, "Information for Contributors to Journals of the AIAA." Failure to use the new address will only delay consideration of your paper.